Desalination and Water Treatment
www.deswater.com

doi: 10.1080/19443994.2015.1033466

57 (2016) 9845–9858
May

Taylor & Francis
Taylor & Francis Group

Evaluation of electrochemical peroxidation (ECP) process variables for removal of co-complex dye using a central composite design

Hakan Pekey

Department of Environmental Engineering, Kocaeli University, Kocaeli 41380, Turkey, email: hpekey@gmail.com

Received 21 February 2014; Accepted 19 March 2015

ABSTRACT

In this study, electrochemical peroxidation was employed to remove color and total organic carbon (TOC) from co-complex (acid yellow 194) dye using iron electrodes in a batch-mode operation. The effects and relationships of the process variables were evaluated, and optimizations were carried out using response surface methodology to maximize removal efficiencies and minimize operating costs in relation to energy, electrode, and chemical (such as H_2O_2) consumptions. The initial pH (2.0–6.0 pH_i), conductivity (500–2,500 μS/cm, k), initial dye concentration (100–800 mg/L, C_0), current density (10–30 A/m^2, j), operating time (4–20 min, t), and dosage of H_2O_2 (2–10 mM or 175–860 μL/L, $M_{H_2O_2}$) were selected as independent variables. The proposed models fit very well with experimental data, evidenced by high R^2 correlation coefficients (>90%). Maximum color removals were 98 and 80% when C_0 was 275 and 625 mg/L, respectively. In contrast, maximum TOC removals were poor (52 and 40% when C_0 was 275 and 625 mg/L, respectively). On the other hand, color and TOC removals were found to be 86 and 33.5%, respectively, at optimum conditions (C_0, 275 mg/L; pH_i 3; k, 1.010 μS/cm; $M_{H_2O_2}$, 5.1 mM; j, 15 A/m; and t, 8.02 min). The calculated operating cost at optimized conditions was 0.647 €/m.

Keywords: Electrochemical peroxidation process; Response surface methodology; Acid yellow 194; Operating cost

1. Introduction

Tanning, the process of treating skins of animals to produce leather, includes various mechanical steps for different product characteristics, such as unhaired, degreased, desalted, soaked, delimed, pickled, tanned, washed, and dyed. The desirable properties of the leather such as appearance, color, and physical and chemical properties are improved during these steps; nevertheless, various solid wastes and wastewater are generated. Especially in the final steps of the tanning process, dyes are added to the wet process to modify the color of the leather, and this process is responsible for a significant volume of wastewater generation containing high concentrations of azo and/or metal complexes dyes. These dyes, when discharged into a water resource, prevent the penetration of sunlight, reduce reoxygeneration capacity, and cause acute and chronic toxicities, aesthetic pollution, and serious health-risk factors; thus, they affect dissolved oxygen concentration, resulting in an anaerobic condition. Therefore, Espantaleon et al. [1] and Piccin et al. [2] reported that purification of this wastewater is a necessary operation to reuse the water in other process steps and/or to meet discharge limits for the natural water environment.

In this study, acid yellow 194 was used as a model dye. It is a co-complex dye characterized by high wash- and light-resistance and a near-zero BOD_5 value, which allows the designation of biodegradation-resistant [3]. The removal of acid yellow 194 is realized through processes such as adsorption [1,2], oxidation by ozone and $(NH_4)_2S_2O_8$ [3], and solar photocatalytic degradation [4].

Espantaleon et al. [1] found from batch experiments that the adsorption capacities of acid yellow 194 are 24.9 and 71.1 mg/g on natural and acid-activated bentonites, respectively. They also demonstrated that its removal is 24.9% using natural clay and 71.1% using acid-activated clay. Maćkowska et al. [3] examined the mechanism of decolorization of dyes using ozone and $(NH_4)_2S_2O_8$ and estimated the number of reaction stages. Saha and Chaudhuri [4] investigated the effectiveness of solar photocatalytic degradation using zinc oxide (0.2–3.0 g/L) at varying dye concentrations; maximum degradation was achieved using 1.5 g/L, degrading 63 to 86% of the initial dye concentration (20 or 50 mg/L) in 15 min.

Traditionally, physico-chemical and biological processes such as flocculation, sedimentation, and activated sludge have been used in the leather industry [2]. The traditional method of purification utilizes a large tank to mix all the effluents generated from the various tanning steps so that some chemical interactions are realized. Nowadays, it is more common to treat each wastewater separately [1,5]. In addition, the conventional treatment methods of tanning wastewaters, such as coagulation/flocculation, membrane separation (ultrafiltration, reverse osmosis), or elimination by adsorption, are not sufficient or cause new issues, such as sludge disposal problems. Therefore, these methods transfer the pollutant from one phase to another (e.g. from liquid to solid phase). Biological treatment methods are not a complete solution to the problem because of the biological resistance of some dyes [6].

On the other hand, advanced methods such as ozonation, electrochemical processes ultrasonic techniques, and photocatalysis have been widely studied for removing dyes [1–3,7–9] It is clear that the processes, such as oxidation, that break down the pollutants into harmless final products, have become important alternatives. However, the disadvantages of oxidation processes, such as long treatment times, high operation and investment costs, and difficulties of process installation, restrict the application of these processes. In such cases, hybrid processes, such as electrochemical peroxidation (ECP) [10], based on oxidation and electrocoagulation (EC) processes, can often bring benefits in terms of the water quality that can be achieved.

The ECP process is a combination of EC and classic Fenton processes, and can bring organics to very low levels by degradation, coagulation, and flotation of pollutants in the wastewaters. In the conventional Fenton process, H_2O_2 and Fe^{2+} are externally applied; whereas in the ECP process, H_2O_2 is added externally and Fe^{2+} is provided by anodic dissolution of sacrificial cast iron anodes (Eq. (1)) in an undivided electrolytic cell. On the other hand, the system simultaneously allows the production of H_2 from H_2O reduction (Eq. (2)) and cathodic regeneration of Fe^{2+} (Eq. (3)) continuously at the inert cathode. During the ECP process, externally added H_2O_2 oxidizes the pollutants in wastewater by generating ·OH radicals (Eqs. (4) and (5)). The regeneration of Fe^{2+} at the inert cathode helps to minimize the extent of parasitic reactions (Eq. (6)) and the accumulation of iron sludge [10–15].

$$Fe \rightarrow Fe^{2+} + 2e^- \quad \text{(Anode)} \tag{1}$$

$$2H_2O + 2e^- \rightarrow H_2 + 2OH^- \quad \text{(Cathode)} \tag{2}$$

$$Fe^{3+} + e^- \rightarrow Fe^{2+} \quad \text{(Cathode)} \tag{3}$$

$$Fe^{2+} + H_2O_2 + H^+ \rightarrow Fe^{3+} + H_2O + {}^{\cdot}OH \quad \text{(In acidic bulk solution)} \tag{4}$$

$$Fe^{3+} + H_2O_2 \rightarrow Fe^{2+} + HO_2^{\cdot} + H^+ \quad \text{(In bulk solution)} \tag{5}$$

$$Fe^{2+} + {}^{\cdot}OH \rightarrow Fe^{3+} + OH^- \quad \text{(In bulk solution)} \tag{6}$$

On the other hand, the formation of metal hydroxide flocs, in the case of a Fe electrode, proceeds according to a complex mechanism which may be simplified [16].

$$Fe^{3+} \Rightarrow \text{monemeric species} \Rightarrow \text{polymeric species} \Rightarrow \text{amorphous } Fe(OH)_3 \tag{7}$$

The formed metal hydroxides destabilize and aggregate the suspended particles or precipitate and adsorb dissolved contaminants (Eq. (7)).

Generally, the effect of particular variables on the removal efficiency of ECP was examined by holding other variables constant in wastewater treatment studies. However, this approach does not take into account the interactions between variables. Response surface methodology (RSM) is a powerful statistical-based technique for modeling complex systems (such as ECP), evaluating the simultaneous effects of several

factors (independent variables), thus finding optimum conditions for the desirable responses (dependent variables). In addition to analyzing the effects of independent variables, RSM also generates a mathematical model that can be used to predict the responses of a system to any new condition [17–20].

The originality/novelty of this study is the application of RSM as a tool to minimize the operational cost (OC) of ECP and maximize its removal efficiencies. To date, RSM has not been used as a modeling and optimization tool for the ECP treatment of co-complex dyes from wastewater, taking into account the effects of process-independent variables such as pH_i, k, C_0, j, t, and $M_{H_2O_2}$ as well as process responses such as process costs, and extent of color and total organic carbon (TOC) removal. In particular, the process costs, which include electrode, energy, and chemical consumption, are generally high for ECP and restrict its application in working wastewater treatment systems. Thus, a cost-driven approach of optimization must be taken.

Considering the above factors, the aims of this study were to investigate the removal of a co-complex dye from wastewater using ECP while minimizing OC related to energy, electrode, and H_2O_2 consumption.

2. Materials and methods

2.1. Wastewater sample preparation and analytical methods

The selected model dye, acid yellow 194, is an azo 1:2 di-sulphonated co-complex dye [1], which is commonly used in the tanning industry during dyeing processes. The commercial acid yellow 194 dye (CAS No. 85959-73-5; MW, 965.9 g/mol; commercial name, Baygenal Yellow Brown 3G) was supplied by the SUMPA Company from Turkey. Fig. 1 shows the chemical structure of the dye [2].

ECP was performed using synthetic dye solutions at concentrations and conductivities close to those observed in tanning wastewater. Acid yellow 194 dye concentrations were chosen in the range of 100–800 mg/L to simulate wastewater concentrations seen in the field and used in published studies [7]. TOC was determined by combustion at 680°C using a non-dispersive IR source (Shimadzu, TOC-L model). Conductivity of the solution was adjusted to 500–2,500 μS/cm using Na_2SO_4. This concentration of salt is quite common in the industry for fixing color [21,22]. Tanneries generate sulfate-rich wastewaters because of the use of large amounts of sulfuric acid and sulfide in the dehairing process, and both are oxidized to sulfate before discharge [8]. Therefore, in this study, use of Na_2SO_4 was preferred over NaCl to adjust the conductivity.

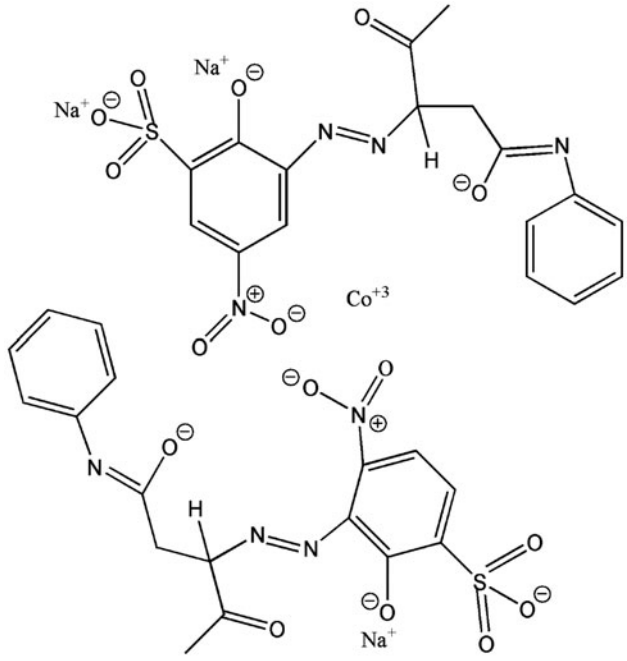

Fig. 1. The chemical structure of acid yellow 194 dyes [2].

In the literature, the removal efficiency of acid yellow 194 was determined using spectrophotometry at 402 [1] or 475 nm [2]. However, in this study, 530 nm was found to be more linear in the 100–800 mg/L range (Fig. 2) at pH between 2 and 10. Therefore, color content was measured at 530 nm using a UV–vis spectrophotometer (Perkin–Elmer 550 SE). The pH was adjusted using 1 N H_2SO_4 or 1 N NaOH and was measured using a pH meter (WTW; Inolab pH 720).

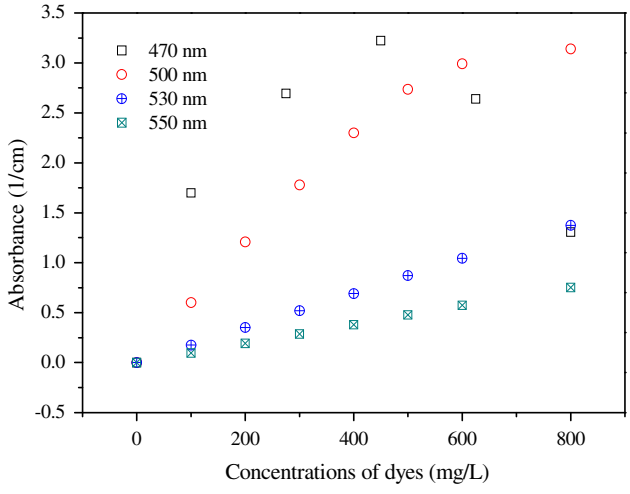

Fig. 2. Calibration graph of acid yellow 194 at various concentrations and wavelengths.

2.2. Experimental setup and procedure

ECP was performed in a batch electrolytic reactor made from Plexiglas and measuring 100 mm × 100 mm × 130 mm (Fig. 3). In general, less Fe was needed in ECP than in EC, and for this reason, only two iron electrodes (purity > 99.5%), effectively measuring 80 mm × 50 mm × 3 mm, were used. The total effective area of the electrodes was 80 cm^2, and electrodes were situated 30 mm apart from each other.

Before each run, organic impurities were removed from the electrode surface by washing with acetone, and the surface oxide layer was removed by dipping it in a freshly prepared mixture of 100 cm^3 35% HCl and 200 cm^3 of a hexamethylenetetramine [$(CH_2)_6N_4$] aqueous solution (2.80%) for 5 min. For each run, 800 cm^3 of synthetic dye solution was placed in the ECP reactor and mixed at 300 rpm. Conductivity and pH were adjusted to the desired value, and the electrodes were inserted in place, after which j was adjusted using a digital DC power supply (TDK-Lambda Genesys model; 50 V-30A) operated in galvanostatic mode. Each run began with the addition of the desired amount of H_2O_2 [23]. The independent variable ranges and levels were determined based on the preliminary experiments. Temperature was not selected as a parameter and was therefore kept constant at 25˚C. At the completion of each run, the electrodes were washed thoroughly with water to remove any solid residues on the surfaces before drying.

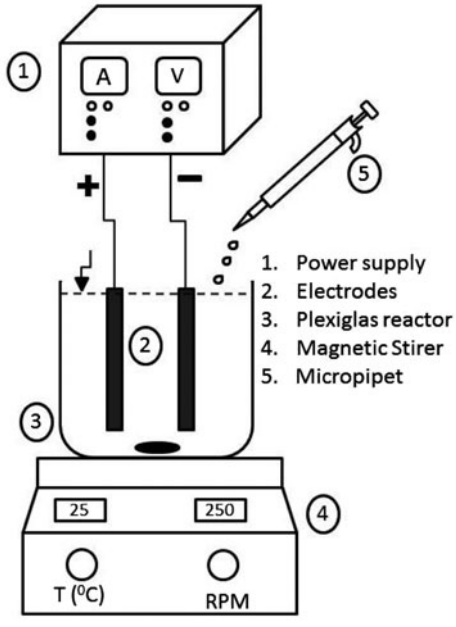

Fig. 3. Schematic diagram of the experimental set-up.

2.3. Toxicity test procedure

Toxicity tests were performed according to the BiotoxTM flash method (Aboatox Oy, Turku Finland), which is based on the bioluminescent response of *Vibrio fischeri* bacteria and incorporates an automatic correction for color and turbidity [24–26]. Luminescence was measured using a high performance Sirius Luminometer, and light output was recorded automatically by FB12 software (Berthold Detection Systems, Pforzheim, Germany). Prior to measurement, freeze-dried *V. fischeri* were re-hydrated in reagent diluent (2% NaCl) at 4˚C for at least 30 min and then stabilized at 15˚C for approximately 1 h in a dry cooling block. The samples were prepared by mixing 9 mL sample with 1 mL 20% NaCl and adjusting the pH to 7.0 ± 0.2 if the sample pH was not between 6.0 and 8.5. The samples were subsequently diluted with 2% NaCl solution to obtain a dilution series (1:2, 1:4, 1:8, 1:16, 1:32, and 1:64). Toxicity measurements were performed by initially placing 300 µL diluted sample into luminometer cuvettes (Sarstedt 55.476) and incubating at 15˚C for at least 10 min. Following introduction into the Sirius Luminometer, 300 µL bacterial suspension was automatically injected into the sample, and bioluminescence was measured, and then repeated after 30 min so that the relationship between end point toxicity and peak toxicity could be elucidated. A correction factor was applied based on the response obtained from the non-toxic reference sample (2% NaCl). The inhibition percentage and the EC20 and EC50 values were calculated according to the ISO standard method 11348-3 [27], where the initial luminescence reading is replaced with the peak value observed immediately after the addition of bacteria to the sample.

2.4. Experimental design and data analysis

In this study, RSM was used in the experimental design, and the composite central design (CCD) was used to fit a model using a least-squares technique. Design Expert 7.1.3 software (trial version) was used for the statistical design and data analysis and was performed in duplicate. The three most important operating variables, pH_i, k, C_0, j, t, and $M_{H_2O_2}$, were selected as independent variables. In addition, TOC, color, and OC were selected as system responses.

The CCD was applied for experimental planning comprising 2^6 full factorial designs. Ten additional runs were replicates of the central point. Analysis of variance (ANOVA) was used for graphical analyses of the data to obtain interactions between the process variables and the responses.

2.5. Operating cost

Operating cost of an ECP process primarily includes electrodes, energy, chemicals (such as H_2O_2 and solutions used for pH adjustment), labor, maintenance, sludge dewatering and disposal, and fixed costs. In this study, energy, electrode, and chemical material costs were used, assuming they are the major cost items:

$$\mathrm{OC}\left(\frac{€}{m^3}\right) = aELC + bENC + cCC \tag{8}$$

where ENC is energy consumption (kWh/m^3), ELC is electrode consumption (kg/m^3), and CC is the consumption quantity of chemicals (kg/m^3). Prices provided in the Turkish market in February 2014 for a and b were 0.072 € kW/h for electrical energy and 0.85 €/kg for Fe electrode material. The variable c represents chemical consumption (kg/m^3), such as NaOH (0.73 €/kg) and H_2SO_4 (0.29 €/kg) for pH adjustment and 1.22 €/kg for H_2O_2 [11]. Costs for electrical energy (kWh/m^3) in Eq. (9) and electrode consumption (kg/m^3) were calculated from Faraday's law in Eq. (10):

$$ENC = \frac{U \times i \times t_{EC}}{v} \tag{9}$$

$$ELC = \frac{i \times t_{EC} \times M_w}{z \times F \times v} \tag{10}$$

where U is cell voltage (V), i is current (A), t_{EC} is operating time (s), v is volume (m^3) of wastewater, M_w is the molecular mass of iron (55.845 g/mol), z_{Fe} is the number of electron transferred (2), and F is Faraday's constant (96,487 C/mol).

3. Results and discussion

3.1. Statistical analysis

RSM is a collection of mathematical and statistical techniques and is used for improving and optimizing processes while allowing the evaluation of interactions between independent and dependent (response) variables. Generally, it uses an experimental design such as CCD to fit a model using a least-squares technique [17,18,28]. It is also possible to represent independent process parameters in quantitative forms:

$$y = f(x_1, x_2, x_3, \ldots, x_n) \pm \varepsilon \tag{11}$$

where y is the response (yield), f is the response function, ε is the experimental error, and x_1, x_2, $x_3, \ldots, x_n$ are independent parameters.

Using ANOVA, the interactions between process variables and responses were evaluated, and the quality of fit of a polynomial model was expressed using the coefficient of determination, R^2. Its statistical significance was checked using the Fisher F-test. The model's terms were evaluated using p values (probability) at a 95% confidence level. The ANOVA results showed that 2-factor interactions (2FI) for color and TOC removal efficiency were appropriate (Table 1) because of the lowest p values and the highest and similar R^2 values (adjusted and predicted R^2). As seen in Table 1, both the quadratic and linear models are appropriate for OC: The more basic one was selected.

The appropriate highest order polynomial allows significance of the additional terms, ensuring the model is not aliased. Values of "Prob > F" that were lower than 0.05 indicate that the terms were significant at a probability level of 95%. In this case, x_1, x_2, x_4, x_5, x_6, $x_1 \times x_2$, $x_1 \times x_4$, and $x_2 \times x_4$ were significant for color removal; x_1, x_2, x_3, x_4, x_5, x_6, $x_1 \times x_2$, and $x_2 \times x_4$ were significant for TOC removal; and x_2, x_3, x_4, x_5, and x_6 were significant for OC (Table 2).

By plotting the expected response of y, a surface known as the response surface is obtained. The form of f is unknown and may be very complicated. Thus, RSM aims to approximate f using a polynomial of suitable order. The linear order regression model (Eq. (12)) and 2FI (Eq. (13)) for predicting the optimal conditions can be expressed:

$$y = \beta_0 + \sum_{i=1}^{k} \beta_i x_i + \varepsilon \tag{12}$$

$$y = \beta_0 + \sum_{i=1}^{k} \beta_i x_i + \sum_{i=1}^{k-1} \sum_{j=1}^{k} \beta_{ij} x_i x_j + \varepsilon \tag{13}$$

where the predicted response y is correlated to the regression coefficients, that is, the intercept (β_0), linear coefficients (β_1, β_2, β_3), and interaction coefficients (β_{12}, β_{12}, β_{23}). The variable k is the number of factors studied and optimized in the experiment, and ε is the random error. In some cases, the suggested models can be modified by deleting insignificant terms to develop ANOVA results. In this study, the modified 2FIs for color removal and OC were obtained by using only significant model terms (Table 2). Thus, modified models fit very well with the experimental data (for instance, R^2 increased from 0.839 to 0.900 for color

removal by modifying the model) compared to unmodified models (Tables 1 and 3).

The estimated coefficients of functions were obtained by modifying models. They are given in Eq. (14) for color removal, Eq. (15) for TOC removal, and Eq. (16) for OC.

For color removal:

$$y_{Re,Color} = +34.97 - 12.90 \times x_1 - 21.42 \times x_2 + 13.63 \times x_4 - 4.59 \times x_5 - 6.23 \times x_6 + 12.08 \times x_1 \times x_2 + 3.47 \times x_1 \times x_4 - 9.06 \times x_2 \times x_4 \quad (14)$$

For TOC removal:

$$y_{Re,TOC} = +16.57 - 4.23 \times x_1 - 5.87 \times x_2 - 1.09 \times x_3 + 5.16 \times x_4 - 2.11 \times x_5 - 2.35 \times x_6 + 4.42 \times x_1 \times x_2 - 1.85 \times x_2 \times x_4 \quad (15)$$

For OC:

$$y_{OC} = +0.76 - 0.015 \times x_2 - 3.226.10^{-3} \times x_3 + 0.23 \times x_4 + 0.015 \times x_5 + 0.016 \times x_6 \quad (16)$$

A positive and negative sign in front of the terms referred to a synergistic effect and antagonistic effect, respectively. For instance, C_0 (x_1), pH_i (x_2), k (x_3), j (x_5), and t (x_6) had a negative influence on color removal. However, $M_{H_2O_2}$ (x_4) had a positive influence on color removal and a negative influence on OC (€/m^3).

3.2. The effects of variables on removal efficiencies

In this study, CCD was used as the experimental design, and a total of 86 runs were performed (Table 4) for examination of the effects of variables on removal efficiencies and OC.

To examine the effects of all factors on responses (removal efficiencies and OC), a perturbation plot shows how the response changes as each factor moves from the chosen reference point when all other factors were held constant at the reference value [29]. The effects of experimental factors on removal efficiencies of color and TOC are shown in Fig. 4. As seen, a reference point was chosen at the middle of the design space. As mentioned in Section 3.1, C_0 (x_1), pH_i (x_2), j (x_5), and t (x_6) had a negative influence on color and TOC removals. However, $M_{H_2O_2}$ (x_4) had a positive influence on color and TOC removals and a negative influence on OC (€/m^3).

As expected, increasing C_0 decreased color and TOC removal efficiencies. When all factors were held constant except for C_0 (runs 6, 9, and 12), color removal efficiencies were 25.3, 38.0, and 76.0% when C_0 values were 800, 450, and 100 mg/L of C_0, respectively. In the same runs, TOC removal efficiencies were 10, 17, and 28%, respectively. The reason for this phenomenon is that increasing C_0 increases the number of dye molecules with stable $^{\cdot}OH$, and therefore, the removal rate is slowed.

When all factors were held constant except for pH (runs 21, 9, and 80), color removal efficiencies were

Table 1
ANOVA results for the models of color, TOC, and OC

Source	Sum of squares	[a]df	Mean square	Sequential p-value	Lack of fit p-value	[a]Adj. R^2	[a]Pred. R^2	Results
Color removal (%)								
Linear	22,717	70	324	<0.0001	0.0756	0.703	0.668	
2FI	6,909	55	125	<0.0001	0.5981	0.876	0.839	Suggested
Quadratic	5,730	49	116	0.1520	0.6496	0.883	0.814	
TOC removal (%)								
Linear	2,173	70	31.05	<0.0001	0.0094	0.7244	0.6905	
2FI	575.81	55	10.47	<0.0001	0.2533	0.9030	0.8688	Suggested
Quadratic	493	49	10.07	0.0466	0.5257	0.9068	0.8445	
OC (€/m^3)								
Linear	0.008	70	0.0001	<0.0001	<0.0001	0.998	0.998	Suggested
2FI	0.006	55	0.0001	0.2825	<0.0001	0.998	0.998	
Quadratic	0.003	49	<0.0001	<0.0001	<0.0001	0.999	0.997	Suggested

[a]df: degree of freedom, Adj: adjusted and Pred: predicted.

Table 2
ANOVA results for terms of color, TOC, and OC

	Color removal (%)			TOC removal (%)			Cost (€/m^3)		
Source	Sum of squares	df	Prob > F	Sum of squares	df	Prob > F	Sum of squares	df	Prob > F
Model	78,574	21	<0.0001	8,171	27	<0.0001	3.89	27	<0.0001
$x_1 = C_0$ (mg/L)	11,974	1	<0.0001	1,290	1	<0.0001	0.00012	1	0.167
$x_2 = pH_i$	33,050	1	<0.0001	2,482	1	<0.0001	0.016	1	<0.0001
$x_3 = k$ (μS/cm)	82	1	0.4238	85	1	0.0040	0.0008	1	0.0006
$x_4 = M_{H_2O_2}$	13,385	1	<0.0001	1915	1	<0.0001	3.84	1	<0.0001
$x_5 = j$ (A/m^2)	1,480	1	<0.001	319	1	<0.0001	0.016	1	<0.0001
$x_6 = t$ (min)	2,793	1	<0.0001	397	1	<0.0001	0.019	1	<0.0001
$x_1 \times x_2$	9,333	1	<0.0001	1,249	1	<0.0001			
$x_1 \times x_3$	38	1	0.5833	16	1	0.1943			
$x_1 \times x_4$	768	1	0.0166	35	1	0.0579			
$x_1 \times x_5$	49	1	0.5346	3	1	0.5900			
$x_1 \times x_6$	9	1	0.7859	23	1	0.1260			
$x_2 \times x_3$	101	1	0.375	1	1	0.8124			
$x_2 \times x_4$	5,257	1	<0.0001	219	1	<0.0001			
$x_2 \times x_5$	53	1	0.5175	5	1	0.4905			
$x_2 \times x_6$	30	1	0.6238	1	1	0.7613			
$x_3 \times x_4$	46	1	0.5467	8	1	0.3787			
$x_3 \times x_5$	16	1	0.7226	22	1	0.1360			
$x_3 \times x_6$	29	1	0.6309	12	1	0.2598			
$x_4 \times x_5$	2	1	0.9121	1	1	0.7672			
$x_4 \times x_6$	62	1	0.4872	1	1	0.7112			
$x_5 \times x_6$	8	1	0.7946	1	1	0.7567			

Table 3
ANOVA results for the modified models of color, TOC, and OC

	Color removal (%)	TOC removal (%)	OC (€/m^3)
Std. Dev.	10.61	3.16	9.875×10^{-3}
Mean	34.97	16.57	0.76
C.V. (%)	30.34	19.05	1.30
PRESS	10,592.89	954.33	8.90×10^{-3}
R^2	0.900	0.912	0.998
Adj. R^2	0.890	0.903	0.998
Pred. R^2	0.878	0.891	0.998
Adeq. precision	34.764	41.559	327.941

Notes: Std. Dev: standard deviation, CV: coefficient of variance, PRESS: predicted residual error sum of squares, Adj: adjusted, Pre: predicted, and Adeq. precision: adequate precision.

61.4, 38.0, and 10.1% when pH_i values were of 2, 4, and 6, respectively. In the same runs, TOC removal efficiencies were 21.0, 17, and 9.1%, respectively. In this study, increasing pH_i from 2 to 6 decreased the removal efficiency (Fig. 4) as expected. We suspect that the dominant removal mechanism is oxidation at low pH and coagulation at high pH, and these results agree with the literature [30–33]. For an effective Fenton oxidation, pH_i should be adjusted to low values; generally, an optimum pH range for wastewater treatment using Fenton oxidation is between 2 and 4 [30]. A high concentration of $^{\cdot}OH$, which is the second-strongest oxidizer, carrying an oxidation potential of 2.80 V (fluorine has an E_0 of 3.06 V), is expected to be produced from the Fenton's reaction within this range [31,32]. This high potential of $^{\cdot}OH$ radicals enables the attack and decomposition of the dye molecules. At high pH_i (especially at 6 in this study), near the effective pH_i in EC systems, color and TOC removal efficiencies are relatively lower than in others. However, the effective pH_i range in EC systems is generally reported to be between 4 and 6 in the literature, and

Table 4
The experimental and calculated results

	C_0 (mg/L)	pH_i	k (μS/cm)	H_2O_2 (mM)	j (A/m^2)	t (min)	Fe (mM)	pH_f	Color Re. (%)	TOC Re. (%)	OC (€/m^3)
1	625	3	1,000	8.0	25	8	0.50	3.23	70.5	20	1.005
2	275	3	2,000	8.0	15	16	0.60	3.64	97.2	33.1	1.005
3	625	5	2,000	4.0	25	8	0.50	4.91	9.7	7.2	0.503
4	450	4	1,500	6.0	20	12	0.60	4.76	27.8	15	0.745
5	275	3	1,000	4.0	25	16	0.99	4.56	57.6	20.3	0.594
6	800	4	1,500	6.0	20	12	0.60	4.21	25.3	10	0.745
7	275	3	1,000	4.0	25	8	0.50	3.57	72.3	25.9	0.547
8	450	4	1,500	6.0	10	12	0.30	4.60	32.3	20.2	0.719
9	450	4	1,500	6.0	20	12	0.60	4.29	38.0	17	0.746
10	625	3	2,000	4.0	15	8	0.30	3.50	14.4	8.2	0.519
11	275	3	1,000	8.0	15	8	0.30	3.16	96.4	40	0.985
12	100	4	1,500	6.0	20	12	0.60	4.23	76.0	28	0.753
13	625	3	1,000	4.0	15	8	0.30	3.47	21.6	13.3	0.521
14	450	4	500	6.0	20	12	0.60	4.60	32.3	20	0.759
15	625	5	2,000	8.0	25	16	0.99	5.73	8.9	7.8	1.004
16	275	5	1,000	8.0	15	8	0.30	3.67	67.7	26	0.951
17	625	5	1,000	8.0	25	8	0.50	4.89	17.6	14	0.970
18	275	5	2,000	4.0	15	8	0.30	5.18	20.4	10	0.485
19	625	5	1,000	8.0	15	16	0.60	5.33	17.7	14	0.973
20	275	3	1,000	4.0	15	16	0.60	3.98	63.4	27	0.548
21	450	2	1,500	6.0	20	12	0.60	2.26	61.4	20.9	1.511
22	275	3	1,000	8.0	15	16	0.60	3.75	96.6	40	1.010
23	625	5	1,000	4.0	15	16	0.60	5.22	10.1	8.2	0.511
24	275	3	2,000	4.0	15	16	0.60	4.04	67.5	23	0.542
25	450	4	1,500	6.0	20	12	0.60	4.96	20.0	19	0.745
26	625	3	2,000	8.0	25	8	0.50	3.20	66.8	22.2	0.999
27	625	5	2,000	4.0	15	8	0.30	4.97	12.6	11	0.485
28	625	3	1,000	8.0	15	16	0.60	3.32	60.7	19.6	1.007
29	275	3	2,000	8.0	25	8	0.50	3.33	97.2	37.4	1.000
30	275	3	2,000	8.0	25	16	0.99	3.68	93.6	29.1	1.041
31	625	3	2,000	4.0	25	8	0.50	3.67	7.3	2	0.536
32	275	5	1,000	8.0	15	16	0.60	5.51	20.4	16	0.975
33	625	3	2,000	4.0	15	16	0.60	3.24	−9.6	2	0.541
34	625	5	2,000	4.0	15	16	0.60	5.53	12.5	9.5	0.507
35	625	3	2,000	8.0	15	8	0.30	3.01	79.7	26	0.981
36	625	3	1,000	4.0	15	16	0.60	3.87	−3.7	3	0.544
37	275	5	1,000	4.0	15	16	0.60	5.70	8.0	5	0.514
38	625	3	1,000	8.0	15	8	0.30	3.08	79.5	30	0.983
39	450	4	1,500	6.0	20	4	0.20	4.40	29.5	20.2	0.715
40	625	5	1,000	4.0	25	8	0.50	5.05	8.8	6	0.509
41	275	3	1,000	4.0	15	8	0.30	3.28	81.3	36	0.523
42	275	5	2,000	4.0	25	8	0.50	5.32	8.0	7	0.504
43	450	4	1,500	6.0	20	12	0.60	3.82	60.9	20.5	0.746
44	450	4	1,500	6.0	20	12	0.60	4.35	32.6	22	0.746
45	450	4	1,500	6.0	30	12	0.90	4.94	22.2	15	0.778
46	275	5	1,000	4.0	25	8	0.50	5.23	13.6	7	0.512
47	275	5	2,000	4.0	25	16	0.99	5.59	−14.0	1	0.544
48	275	3	1,000	8.0	25	16	0.99	3.73	98.1	35	1.053
49	625	3	2,000	4.0	25	16	0.99	4.14	−13.6	2	0.577
50	625	5	1,000	4.0	25	16	0.99	5.47	3.1	2	0.553
51	625	3	1,000	8.0	25	16	0.99	3.65	47.3	20	1.048

(*Continued*)

Table 4 (*Continued*)

	C_0 (mg/L)	pH_i	k (μS/cm)	H_2O_2 (mM)	j (A/m^2)	t (min)	Fe (mM)	pH_f	Color Re. (%)	TOC Re. (%)	OC (€/m^3)
52	625	5	2,000	8.0	15	16	0.60	5.45	15.5	14	0.968
53	275	3	2,000	4.0	25	8	0.50	3.55	70.8	25	0.538
54	625	3	1,000	4.0	25	16	0.99	4.13	−14.9	1	0.585
55	275	3	2,000	8.0	15	8	0.30	3.17	97.2	36	0.982
56	275	5	2,000	8.0	25	8	0.50	5.12	16.1	14	0.966
57	275	5	2,000	8.0	25	16	0.99	5.61	−3.9	3	1.006
58	275	5	2,000	8.0	15	8	0.30	5.20	21.1	13.6	0.948
59	625	5	2,000	8.0	15	8	0.30	5.19	10.8	10.8	0.948
60	275	5	1,000	4.0	25	16	0.99	6.68	−6.9	2	0.558
61	275	5	2,000	8.0	15	16	0.60	5.35	14.4	13	0.969
62	625	3	2,000	8.0	15	16	0.60	3.34	60.2	22	1.004
63	275	5	1,000	8.0	25	16	0.99	5.92	2.8	2	1.018
64	625	5	2,000	8.0	25	8	0.50	4.94	14.4	13	0.965
65	450	4	1,500	6.0	20	12	0.60	4.71	28.2	14	0.746
66	625	5	1,000	4.0	15	8	0.30	4.93	14.5	11	0.487
67	450	4	2,500	6.0	20	12	0.60	3.78	53.9	18	0.745
68	275	5	1,000	8.0	25	8	0.50	5.13	20.0	18	0.974
69	625	5	2,000	4.0	25	16	0.99	5.58	−1.5	1	0.542
70	275	3	1,000	8.0	25	8	0.50	3.35	97.2	38	1.007
71	450	4	1,500	6.0	20	12	0.60	4.64	31.4	19	0.747
72	450	4	1,500	6.0	20	12	0.60	4.77	27.0	15.5	0.747
73	450	4	1,500	10.0	20	12	0.60	3.76	71.1	30	1.209
74	450	4	1,500	6.0	20	12	0.60	5.15	22.2	18.7	0.748
75	625	3	1,000	4.0	25	8	0.50	3.83	6.5	7	0.542
76	625	3	2,000	8.0	25	16	0.99	3.63	47.6	20	1.040
77	450	4	1,500	6.0	20	12	0.60	4.81	25.3	20	0.748
78	450	4	1,500	6.0	20	20	0.99	5.34	19.4	17	0.782
79	625	5	1,000	8.0	25	16	0.99	5.52	12.3	12	1.015
80	450	6	1,500	6.0	20	12	0.60	5.86	10.1	9.1	0.744
81	275	5	2,000	4.0	15	16	0.60	5.78	5.0	3.5	0.508
82	450	4	1,500	2.0	20	12	0.60	5.11	20.8	10	0.286
83	625	5	1,000	8.0	15	8	0.30	4.75	19.7	18.6	0.949
84	275	3	2,000	4.0	15	8	0.30	3.28	80.0	28	0.520
85	275	5	1,000	4.0	15	8	0.30	5.17	21.3	12	0.489
86	275	3	2,000	4.0	25	16	0.99	4.55	54.2	20	0.578

the removal mechanism in this pH range was explained as co-precipitation [33]. In this study, the relatively lower color and TOC removal efficiencies observed at high pH_i may be a result of insufficient Fe ions for EC process. The produced Fe ions, according to Eqs. (1) and (7), are most likely sufficient for the Fenton process but insufficient for coagulation. According to these results, oxidation is the main removal mechanism in this study.

The variables j and t are important parameters for controlling the reaction rate in electrochemical processes such as EC and electro-Fenton processes, as well as ECP [11]. When sacrificial metals (such as Fe or Al) are used as the anode and cathode, it is well known that j and t not only determine the amount of metal species formed by the dissolution of the anode, but also determine the bubble production rate and size, which can influence the treatment efficiency and OC of the system [34]. In our runs, increasing j and t decreased the color and TOC removal efficiencies (Fig. 4). As seen in Table 4, color removal efficiencies were 32.3, 27.8, and 20.2% when j was 10, 20, and 30 (runs 8, 4, and 45), and 29.5, 27.8, and 19.4% when t was 4, 12, and 20 min. (runs 39, 4 and 78), respectively, when all other factors were held constant. A similar trend was observed for TOC efficiencies in the same runs. The removal mechanisms of coagulation and oxidation were therefore shown to be effective in ECP, and amount of metal species played a key role in both of them. The negative effect of increasing j and t is probably based on three reasons: (i) during ECP, increasing j and t increased pH

according to Eq. (2), which inhibits the oxidation process when final pH was outside the effective pH interval of the Fenton's reactions, (ii) recent studies show that increasing the Fe^{2+} can inhibit the degradation rate of the pollutants because of competitive reactions (Eq. (6)) [10,27,29–31], and (iii) when the Fe^{2+} produced at the anode is oxidized by dissolved oxygen in the water, it gives a yellow color to the water that is very similar to that given by acid yellow 194. Probably, the negative removal efficiencies (Table 4) are a result of this resultant yellow color.

Another result derived from Table 4 shows that color and TOC removals were not influenced by k in the chosen range (500–2,500 μS/cm).

It is clear that the main effective variable for color and TOC removal efficiencies in this study was $M_{H_2O_2}$ (Figs. 4 and 5). When all factors are held constant (runs 82, 9, and 73) except for $M_{H_2O_2}$, color removal efficiencies (20.8, 38.0, and 71.1%) and TOC removal efficiencies (10.0, 17.0, and 30.0%) were obtained when $M_{H_2O_2}$ was 2, 6, and 10 mM H_2O_2, respectively. The addition of H_2O_2 proves to increase the production of the main oxidizing agent, $^{\cdot}OH$, as shown in Eq. (4), thus yielding a rapid oxidation of pollutant. In addition, during ECP, pH of wastewater increases according to Eq. (2); however, adding H_2O_2 may block increasing the wastewater pH, according to Eq. (5), by reaction of the newly produced ferric ions (Fe^{3+}) according to Eq. (4). In Fenton-like processes, $[Fe^{2+}]/[H_2O_2]$ ratios are utilized as key operating factors, which are calculated based on Faraday's law and use of H_2O_2 [10,11]. In this study, higher removal efficiencies (>80%) were obtained at higher molar ratios (>13) of $[H_2O_2]/[Fe^{2+}]$ (runs 2, 11, 22, 29, 30, 38, 41, 48, 55, 70, and 84).

In this study, color removal efficiencies were always higher than TOC removal efficiencies (Table 4). During oxidation, oxidants produced during ECP attack and decompose chromophores or bonds between different aromatic rings and functional groups (–OH and $–SO_3H$), which can supply color through absorption of radiant energy in the first step, and if the oxidant is abundant enough, overall degradation is realized. However, low TOC removal efficiencies show that the amount of oxidant produced is not enough for overall degradation of molecules. This result is similar to that seen in other studies that show possible mechanisms for dye degradation through ·OH radicals [35].

3.3. The effects of variables on OC and optimization of ECP

A common characteristic of advanced oxidation processes is the high treatment cost because of the large amount of electrical energy required for function of the apparatus, which is comprised of ultraviolet lamps, ozonizers, ultrasound [36], and electrodes and characterized by high consumption of chemicals and long operation time. Therefore, optimization of ECP through minimized cost and maximized removal efficiencies may allow the application of this system in wastewater treatment.

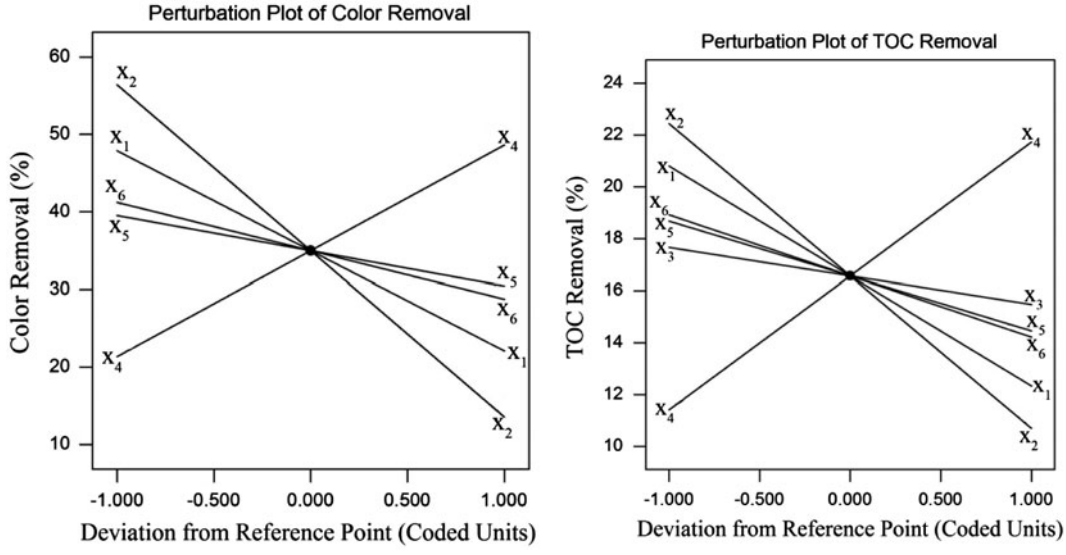

Fig. 4. Perturbation plot of color and TOC removal efficiencies.

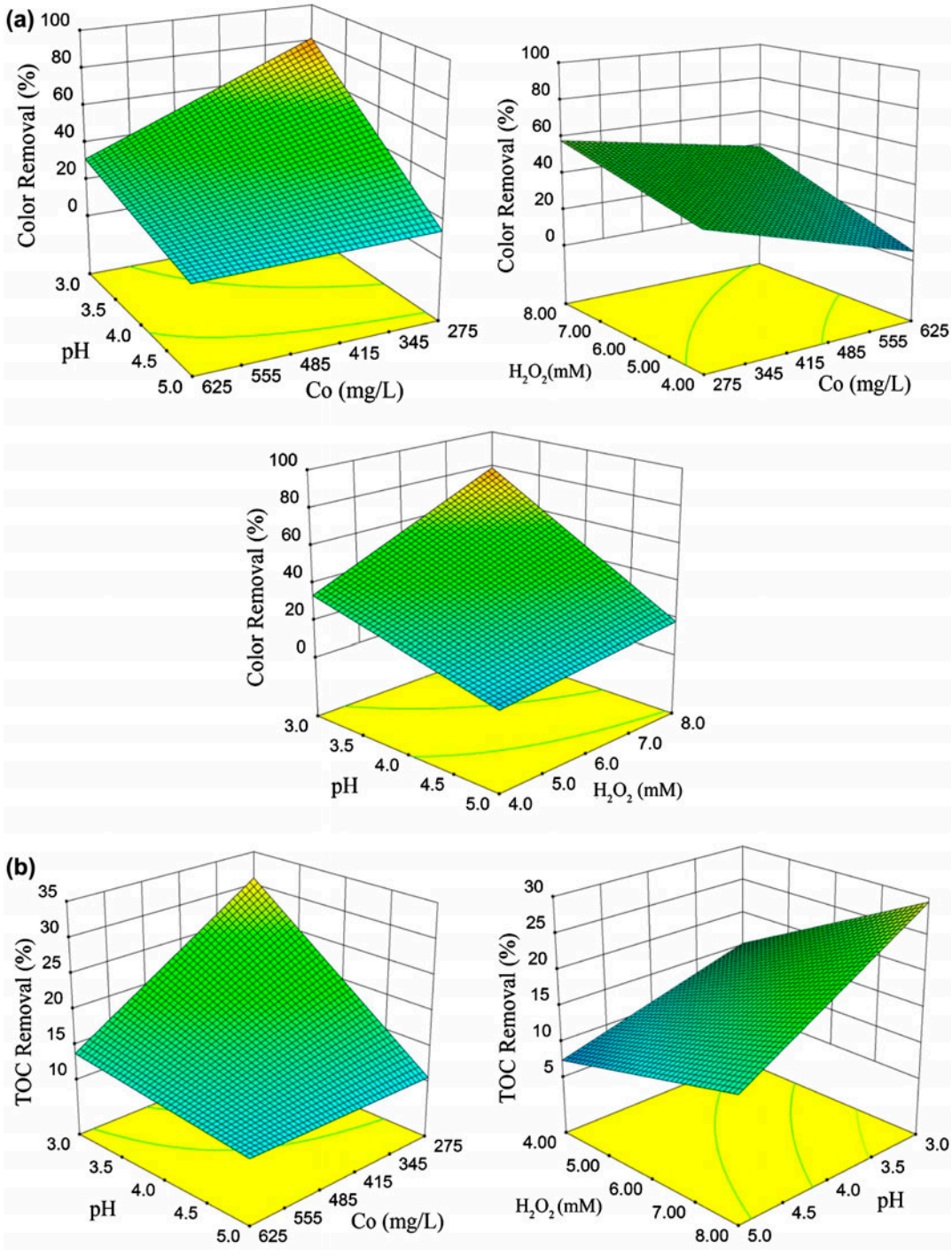

Fig. 5. Effects of the variables on color (a) and TOC (b) removal efficiencies.

The effects of experimental factors on OC are shown in Fig. 6. The variables pH_i (x_2), $M_{H_2O_2}$ (x_4), j (x_5), and t (x_6) had negative influences on OC, whereas C_0 (x_1) and k (x_3) had a positive effect. However, it is clear that the concentration H_2O_2 was a primary factor in OC because of its high cost, possibly limiting ECP in commercial use.

Another interesting observation is that increasing $C_0(x_1)$ caused a relative decrease in OC. This phenomenon can be explained by the increase in

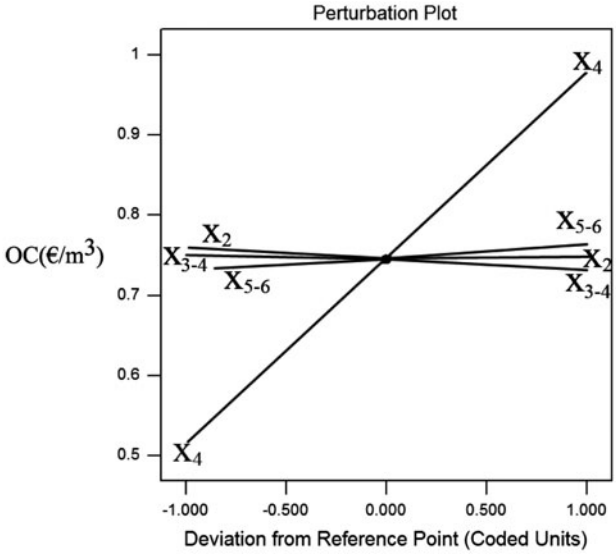

Fig. 6. Effects of the variables on OC using a perturbation plot.

conductivity which leads to a decrease in *ENC* [29], because in ECP, *ENC*, *ELC*, and OC are closely related over potential and time, as described in Eqs. ((9) and (10)). On the other hand, increasing j and t led to increased *ENC*, *ELC*, and OC, as expected according to Eqs. ((3) and (4)). See Fig. 6.

When all factors were held constant, except for j, *ENC* was 0.019, 0.154, and 0.358 (kWh/m^3), and *ELC* was 0.21, 0.42, and 0.63 (kg Fe/m^3) when j was 10, 20, and 30 A/m^2 (runs 8, 44, and 45), respectively. Perturbation plots showed that using added aliquots of sulfuric acid for adjusting pH$_i$ increased OC.

When operating variables were in the pre-determined range, color removal efficiency was maximized and OC was minimized in the RSM model with a desirability of 0.764 (Table 5). Desirability is a multiple response method [28] which reflects the desirable ranges for each response. The desirable ranges are from 0 to 1 (least to most desirable, respectively). Optimization results for the maximum color and TOC removal efficiencies were obtained as 83.8 and 33.5% at C_0 = 275 mg/L, pH$_i$ 3, k = 1.011 μS/cm, $M_{H_2O_2}$ = 5.1 mM, j = 15 A/m^2, and t = 8.0 min in the ECP for the system. The OC of the model at the optimized conditions was 0.644 €/m^3.

3.4. Toxicity studies

Bioassay based on the bioluminescence inhibition of *V. fischeri* is probably the most widely applied bacterial test in wastewater toxicity assessment. Bacterial bioluminescence is attributed to activation of the enzyme luciferase with luciferin. The attenuation of light emitted by bacteria in the presence of a toxicant is related to the inhibition of this reaction [37]. The flash toxicity test was applied to assess the changes in toxicity of raw and treated wastewaters under optimum

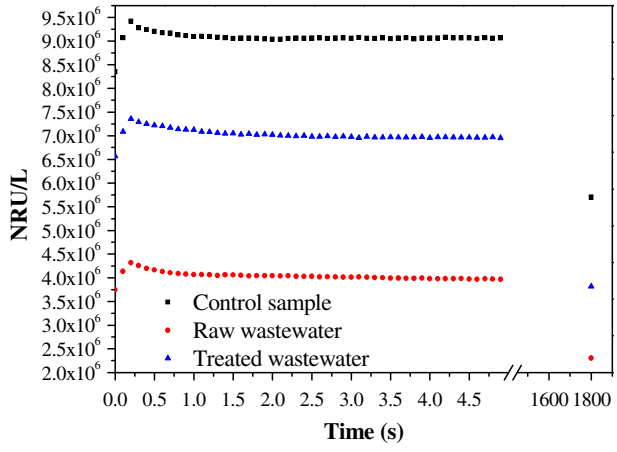

Fig. 7. Luminescence results of raw and treated wastewater.

Table 5
Optimization constraints and results

Name	Goal	Lower limit	Upper limit	Optimization results
x_1: C_0 (mg/L)	In range	275	625	275
x_2: pH$_i$	In range	3	5	3
x_3: k (μS/cm)	In range	1.000	2.000	1.011
x_4: $M_{H_2O_2}$	In range	4	8	5.1
x_5: j (A/m^2)	In range	15	25	15
x_6: t (min)	In range	8	16	8.00
$R_{e,Color}$ (%)	Max.	−14	98	83.8
$R_{e,TOC}$ (%)	Max	1	40	33.5
OC (€/m^3)	Min.	0.286	1.21	0.644
Desirability	Max.	0	1	0.764

experimental conditions. The luminescence values of the control sample (2% NaCl) and treated wastewater are higher than raw wastewater (Fig. 7). However, the raw wastewater did not have a high toxicity value (EC_{20} = 67.42) at this concentration (C_0 = 275 mg/L). Sometimes highly toxic intermediate products can be formed or inserted, and unconsumed chemicals (such as H_2O_2, Fe, etc.) can cause higher toxicity during oxidation. However, the calculated results for treated wastewater (EC_{20} = 52.64) show that there are not a highly toxic intermediate products or toxic effect of unconsumed chemicals during treatment.

4. Conclusions

ECP for color removal of a metal complex dye used as a model for wastewater treatment was investigated on a laboratory scale by using iron electrodes. Our results suggest that the ECP used in this study may be an alternative for the treatment of colored wastewater. Also, this study demonstrated that a RSM and CCD statistical experimental design could give statistically significant results for color removal of metal complex dyes by ECP as well as determine optimum conditions of independent variables with an OC that allows the adjustment of the application to the treatment system. Independent variables and their interactions were found to be effective in color removal using this hybrid technique. The maximum color and TOC removal efficiencies at an OC of 1.053 €/m^3 were found to be 98 and 35.2%, respectively, when C_0 was 2.75 mg/L. However, optimum OC was only 0.644 €/m^3 with satisfactory removal efficiencies (83.8% for color and 33.5% for TOC) when C_0 = 275 mg/L, pH_i = 3, k = 1.011 μS/cm, $M_{H_2O_2}$ = 5.1 mM, j = 15 A/m^2, and t = 8.0 min in the ECP system. The high cost differences between maximum and optimum points show that RSM can be used as a tool to minimize ECP OC.

This study also demonstrated that process parameters such as j, t, pH_i, and amount of H_2O_2 should be taken into consideration for an effective treatment system in the range of the studied parameters, and oxidation is the main removal mechanism found in this study. However, because TOC removal efficiencies were lower than those for color removal, oxidants produced during ECP are shown attack and decompose the azo double bond in the first step and then, if the oxidant is abundant enough, overall degradation is realized.

Although OC is relatively high, it can be applied to non-biodegradable wastewater, such as that created as a by-product of the tanning process. Also, chemicals used in ECP, such as H_2SO_4 and H_2O_2, can be supplied from by-products or wastes of other industries, thus decreasing OC.

References

[1] A.G. Espantaleón, J.A. Nieto, M. Fernandez, A. Marsal, Use of activated clays in the removal of dyes and surfactants from tannery waste waters, Appl. Clay Sci. 24 (2003) 105–110.
[2] J.S. Piccin, C.S. Gomes, L.A. Feris, M. Gutterres, Kinetics and isotherms of leather dye adsorption by tannery solid waste, Chem. Eng. J. 183 (2013) 30–38.
[3] E. Maćkowska, R. Gogolin, W. Dumczal, J. Gaca, Studies of the kinetics of dye decomposition in water solutions, Pol. J. Environ. Stud. 12 (2003) 425–429.
[4] A.K. Saha, M. Chaudhuri, Solar photocatalytic degradation of metal complex azo dyes and treatment of dye house waste, Indian J. Eng. Mater. Sci. 10 (2003) 69–74.
[5] E. Heidemann, Fundamentals of Leather Manufacture, Eduard Roether KG, Darmstadt, 1993.
[6] M.S. Lucas, J.A. Peres, Decolorization of the azo dye reactive black 5 by Fenton and photo-Fenton oxidation, Dyes Pigm. 71 (2006) 236–244.
[7] A. Anastasi, F. Spina, V. Prigione, V. Tigini, P. Giansanti, G.C. Varese, Scale-up of a bioprocess for textile wastewater treatment using *Bjerkandera adusta*, Bioresour. Technol. 101 (2010) 3067–3075.
[8] M.V. Galiana-Aleixandre, J.A. Mendoza-Roca, A. Bes-Piá, Reducing sulfates concentration in the tannery effluent by applying pollution prevention techniques and nanofiltration, J. Cleaner Prod. 19 (2011) 91–98.
[9] C.A. Martínez-Huitle, E. Brillas, Decontamination of wastewaters containing synthetic organic dyes by electrochemical methods: A general review, Appl. Catal., B 87 (2009) 105–145.
[10] E. Brillas, I. Sirés, M.A. Oturan, Electro-Fenton process and related electrochemical technologies based on Fenton's reaction chemistry, Chem. Rev. 109 (2009) 6570–6631.
[11] A. Akyol, O.T. Can, E. Demirbas, M. Kobya, A comparative study of electrocoagulation and electro-Fenton for treatment of wastewater from liquid organic fertilizer plant, Sep. Purif. Technol. 112 (2013) 11–19.
[12] S. Yue, F. Qiyan, L. Xiangdong, Application of response surface methodology to optimize degradation of polyacrylamide in aqueous solution using heterogeneous Fenton process, Desalin. Water Treat. 53 (2015) 1923–1932.
[13] A. Talebi, N. Ismail, T.T. Teng, A.F.M. Alkarkhi, Optimization of COD, apparent color, and turbidity reductions of landfill leachate by Fenton reagent, Desalin. Water Treat. 52 (2014) 1524–1530.
[14] M.I. Badawy, F. El-Gohary, T.A. Gad-Allah, M.E.M. Ali, Treatment of landfill leachate by Fenton process: Parametric and kinetic studies, Desalin. Water Treat. 51 (2013) 7323–7330.
[15] D. Mansour, F. Fourcade, N. Bellakhal, M. Dachraoui, D. Hauchard, A. Amrane, Biodegradability improvement of sulfamethazine solutions by means of an electro-Fenton process, Water Air Soil Pollut. 223 (2012) 2023–2034.

[16] M. Kobya, S. Delipinar, Treatment of the baker's yeast wastewater by electrocoagulation, J. Hazard. Mater. 154 (2008) 1133–1140.
[17] M.J. Anderson, P.J. Whitcomb, RSM Simplified—Optimizing Processes Using Response Surface Methods for Design of Experiments, Productivity Press, New York, NY, 2005.
[18] R.H. Myers, D.C. Montgomery, C.M. Anderson-Cook, Response Surface Methodology: Process and Product Optimization Using Designed Experiments, third ed., Wiley, New Jersey, NJ, 2009.
[19] T. Olmez-Hanci, Z. Kartal, İ. Arslan-Alaton, Electrocoagulation of commercial naphthalene sulfonates: Process optimization and assessment of implementation potential, J. Environ. Manage. 99 (2012) 44–51.
[20] M. Ghanbarzadeh Lak, M.R. Sabour, A. Amiri, Application of quadratic regression model for Fenton treatment of municipal landfill leachate, Waste Manage. 32 (2012) 1895–1902.
[21] P. Ghosh, L.K. Thakur, A.N. Samanta, S. Ray, Electro-Fenton treatment of synthetic organic dyes: Influence of operational parameters and kinetic study, Korean J. Chem. Eng. 29 (2012) 1203–1210.
[22] K. Pratap, A.T. Lemley, Electrochemical peroxide treatment of aqueous herbicide solutions, J. Agric. Food. Chem. 42 (1994) 209–215.
[23] E. Gengec, M. Kobya, Treatment of baker's yeast wastewater by electrocoagulation and evaluation of molecular weight distribution with HPSEC, Sep. Sci. Technol. 48 (2013) 2880–2889.
[24] K. Karlsson, M. Viklander, L. Scholes, M. Revitt, Heavy metal concentrations and toxicity in water and sediment from storm water ponds and sedimentation tanks, J. Hazard. Mater. 178 (2010) 612–618.
[25] J. Lannalainen, R. Juvonen, K. Vaajasaari, M. Karp, A new flash method for measuring the toxicity of solid and colored samples, Chemosphere 38 (1999) 1069–1083.
[26] J. Lappalainen, R. Juvonen, J. Nurmi, M. Karp, Automated color correction method for *Vibrio fischeri* toxicity test. Comparison of standard and kinetic assays, Chemosphere 45 (2001) 635–641.
[27] International Organization for Standardization (ISO), Water Quality—Determination of the Inhibitory Effect of Water Samples on the Light Emission of *Vibrio fischeri* (Luminescent Bacteria Test)—Part 3: Method Using Freeze-dried Bacteria. ISO 11348-3, second ed., Geneva, 2007.
[28] R.H. Myers, D.C. Montgomery, Response Surface Methodology: Process and Product Optimization Using Designed Experiments, Wiley, second ed., New York, NY, 2002.
[29] E. Gengec, M. Kobya, E. Demirbas, A. Akyol, K. Oktor, Electrochemical treatment of baker's yeast wastewater containing melanoidin: Optimization through response surface methodology, Water Sci. Technol. 65 (2012) 2183–2190.
[30] H. Zhang, H.J. Choi, C.-P. Huang, Optimization of Fenton process for the treatment of landfill leachate, J. Hazard. Mater. 125 (2005) 166–174.
[31] B. Boye, M.M. Morième Dieng, E. Brillas, Anodic oxidation, electro-Fenton and photoelectro-Fenton treatments of 2,4,5-trichlorophenoxyacetic acid, J. Electroanal. Chem. 557 (2003) 135–146.
[32] A. Altin, An alternative type of photoelectro-Fenton process for the treatment of landfill leachate, Sep. Purif. Technol. 61 (2008) 391–397.
[33] E. Brillas, B. Boye, I. Sirés, J.A. Garrido, R.M. Rodríguez, C. Arias, P.-L. Cabot, C. Comninellis, Electrochemical destruction of chlorophenoxy herbicides by anodic oxidation and electro-Fenton using a boron-doped diamond electrode, Electrochim. Acta 49 (2004) 4487–4496.
[34] E. Gengec, M. Kobya, E. Demirbas, A. Akyol, K. Oktor, Optimization of baker's yeast wastewater using response surface methodology by electrocoagulation, Desalination 286 (2012) 200–209.
[35] P.K. Malik, S.K. Saha, Oxidation of direct dyes with hydrogen peroxide using ferrous ion as catalyst, Sep. Purif. Technol. 31 (2003) 241–250.
[36] V. Kokkali, Electrochemical peroxidation of contaminated water and assessment of the toxicity using existing and novel bioassays, Ph.D. Thesis, Cranfield University, 2011.
[37] N. Kováts, M. Refaey, B. Varanka, K. Reich, A. Ferincz, A. Ács, Comparison of conventional and *Vibrio fischeri* bioassays for the assessment of municipal wastewater toxicity, Environ. Eng. Manage. 11 (2012) 2073–2076.